

FILE COPY
ESD-TR-76-308

AD/

ESD ACCESSION NO.

DRI Call No.

85881

Copy No.

1 - 2

Project Report

ETS-3

A. S. Friedman

Determination of Specular Reflection
from Cylindrical Satellites
for Electro-optical Surveillance and SOI

8 October 1976

Prepared for the Department of the Air Force
under Electronic Systems Division Contract F19628-76-C-0002 by

Lincoln Laboratory

MASSACHUSETTS INSTITUTE OF TECHNOLOGY

LEXINGTON, MASSACHUSETTS



Approved for public release; distribution unlimited.

AD-A034580

The work reported in this document was performed at Lincoln Laboratory, a center for research operated by Massachusetts Institute of Technology, with the support of the Department of the Air Force under Contract F19628-76-C-0002.

This report may be reproduced to satisfy needs of U.S. Government agencies.

This technical report has been reviewed and is approved for publication.

FOR THE COMMANDER



Raymond L. Loiselle, Lt. Col., USAF
Chief, ESD Lincoln Laboratory Project Office

MASSACHUSETTS INSTITUTE OF TECHNOLOGY
LINCOLN LABORATORY

DETERMINATION OF SPECULAR REFLECTION
FROM CYLINDRICAL SATELLITES
FOR ELECTRO-OPTICAL SURVEILLANCE AND SOI

A. S. FRIEDMAN

Group 94

PROJECT REPORT ETS-3

8 OCTOBER 1976

Approved for public release; distribution unlimited.

LEXINGTON

MASSACHUSETTS

ABSTRACT

Although electro-optical satellite surveillance depends primarily upon diffuse solar reflection, an understanding of specular reflection can lead to enhanced detection and identification capability.

An analysis of the timing and duration of observable specular reflections has been completed for the widely applicable case of the cylindrical satellite. A solution is presented for geosynchronous satellites which includes orbital elements and attitude as parameters. This solution, in turn, is broadened to encompass misalignment of spin axis and symmetry axis.

A realization of the above computation in readily accessible, command-structured format has been developed as a planning aid for the GEODSS Experimental Test System. Samples of its output are provided, which record the occurrence of observable specular reflections in a convenient, easily understood calendrical tabulation.

Predicting the timing and duration of observable specular reflections is of considerable interest in the conduct of electro-optical satellite surveillance. Since a satellite may appear many magnitudes brighter when seen by specularly reflected sunlight than when seen only by diffusely reflected sunlight, this interest is quite understandable. Before providing an explanation of this phenomenon, let us turn to an example.

Figure 1 depicts a strip chart segment containing the optical signature (or light curve) of satellite 83525, as observed on 6 May 1976. The horizontal coordinate represents time, here amounting to a span of 90 s, and the vertical coordinate is proportional to satellite brightness. One function of a GEODSS site is the collection of strip charts such as this for further SOI analysis. An examination of the full strip chart reveals that the satellite is performing some sort of periodic gyration, as evidenced by the light curve's period of 40 s.

In order to assign consistent numerical values to brightness measurements, calibration readings of selected stars of known color and brightness must also be taken. [Figure 3]. This procedure provides values for night sky brightness and atmospheric extinction as well.

Figure 2 shows the light curve of the same satellite, this observation made on 25 March 1976. Comparison with Figure 1 reveals an increase in peak brightness of two magnitudes, which can be attributed to specular reflections. In this example the observations are separated by 42 days, but such an effect could arise in the space of 42 hours or 42 minutes.

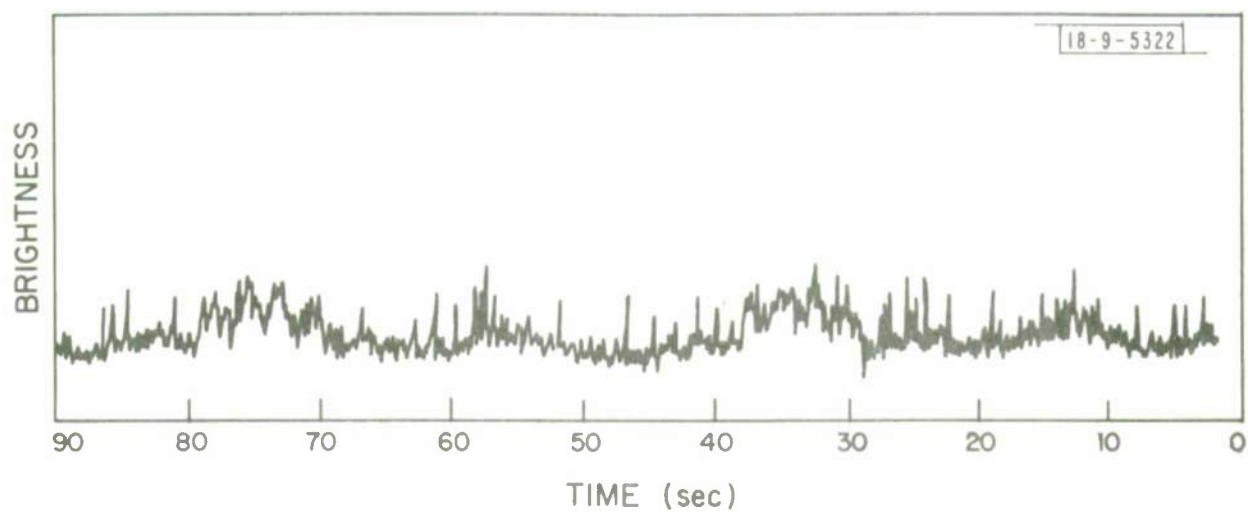


Fig. 1. Light curve of satellite, 83525 6 May 1976

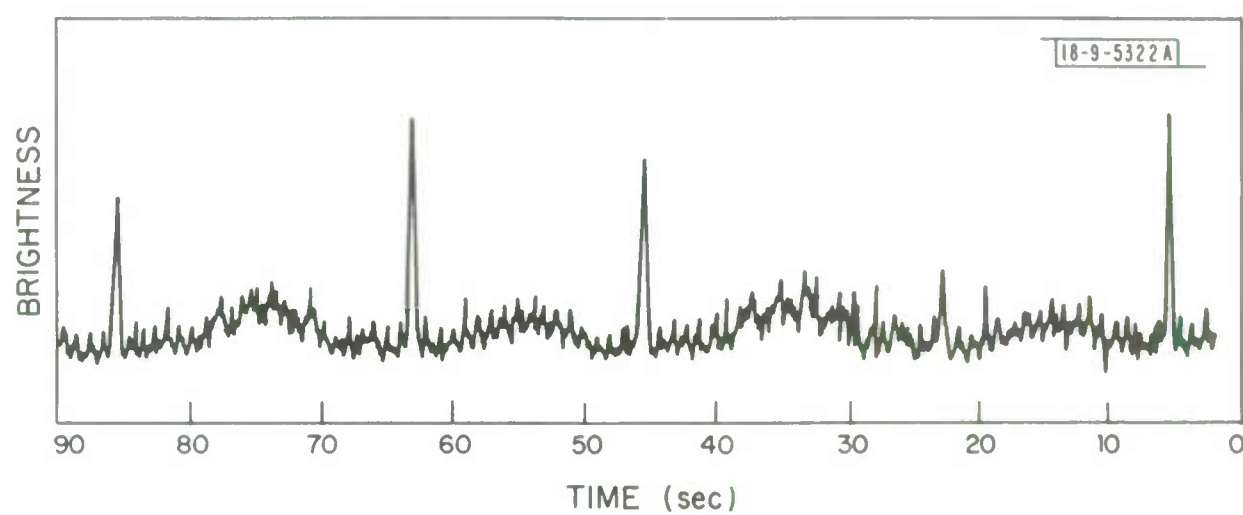


Fig. 2. Light curve of satellite, 83525 25 March 1976

18-9-5326

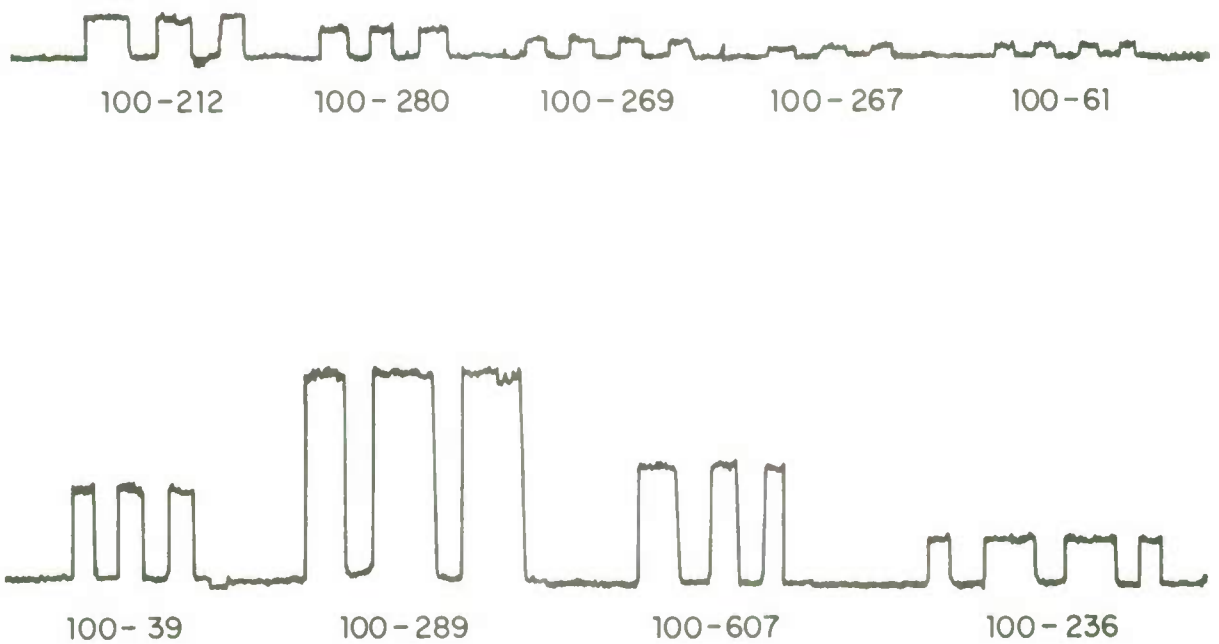


Fig. 3. Light curves, selected Landolt calibration stars

The mission of GEODSS does not include an SOI analysis of the fine structure of light curves, which is the domain of several other Air Force sponsored programs. But a preliminary examination of the light curve for such information as period and average brightness can vitally assist the surveillance role of GEODSS, by confirming the acquisition of a familiar satellite or by providing a means of distinguishing between satellites in the same vicinity. For this reason it is important to understand any phenomenon resulting in an anomalous change in brightness. Furthermore, a mastery of the timing of specular reflections can be a valuable scheduling asset, since maximum brightness should permit minimum search time. An extreme illustration is the case of satellite IMP-6, which was detected electro-optically on 24 October 1973 at a distance of 170,000 km - four times geosynchronous altitude - through the 31-inch telescope at Lowell Observatory. Had specular flashes not been visible, the satellite could not have been seen at all.

After so many repetitions of the term specular reflection, an explanation is now in order. Mirrorlike reflection from a shiny surface is termed specular, as distinguished from so-called diffuse reflection from an unpolished surface. Diffuse reflection is omnidirectional, while specular is limited in extent and consequently more concentrated. A single object may produce reflections of both types. With respect to satellites, it is diffusely reflected sunlight which ordinarily permits optical detection. Specular reflections, even if they occur, will be visible at a particular terrestrial location only when applicable geometric conditions are satisfied.

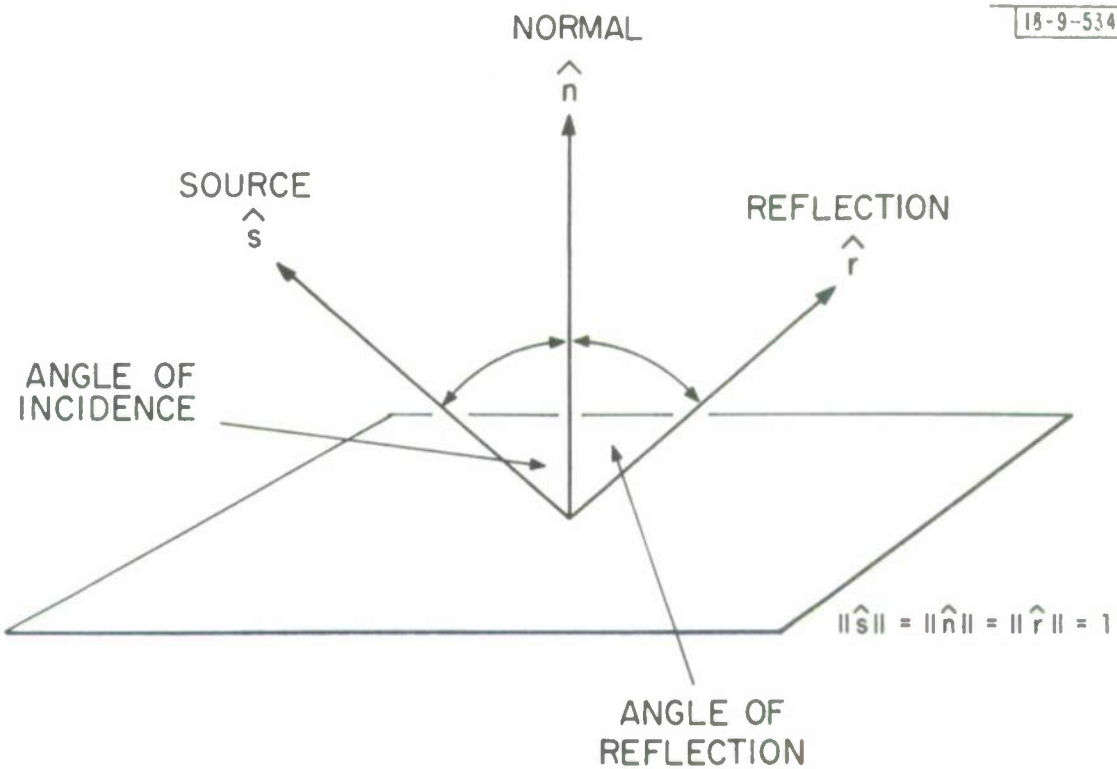
For a flat plate, the rule describing specular reflection is well-known: the angle of incidence equals the angle of reflection. This law is depicted in vectorial form in Figure 4. It may be readily extended to curved surfaces by measuring all angles from the normal at the point of reflection.

The chart in Figure 5 describes the current deployment of geosynchronous satellites launched before 1 January 1976. Observe that the large majority have cylindrical bodies. Such satellites are usually faced with solar cells, which are known to be specular reflectors, and for these a specularly reflecting cylinder serves as a good mathematical model. We will limit our attention to this important category, diagrammed in Figure 6. Light rays incident upon the cylinder from a single direction diverge, after reflection, in a multidirectional configuration whose shape is approximately conical. As seen from a sufficiently great distance, that configuration can be regarded as a perfect right circular cone, coaxial with the cylinder and making the same angle with its axis as does the incoming light. [Figure 7].

In the case of solar illumination, the sun may be considered a remote disk of angular diameter one-half degree. Its reflected light thus constitutes a "thickened" cone, of angular thickness one-half degree, as illustrated in Figure 8. Let us now inquire how these reflections impinge upon the earth.

As a preliminary simplification, Figure 9 depicts a spherical earth and an ideal geosynchronous satellite, cylinder axis parallel to the

18-9-5342



$$\hat{r} = -\hat{s} + 2(\hat{s} \cdot \hat{n})\hat{n}$$

Fig. 4. Specular reflection from a flat plate-vector representation

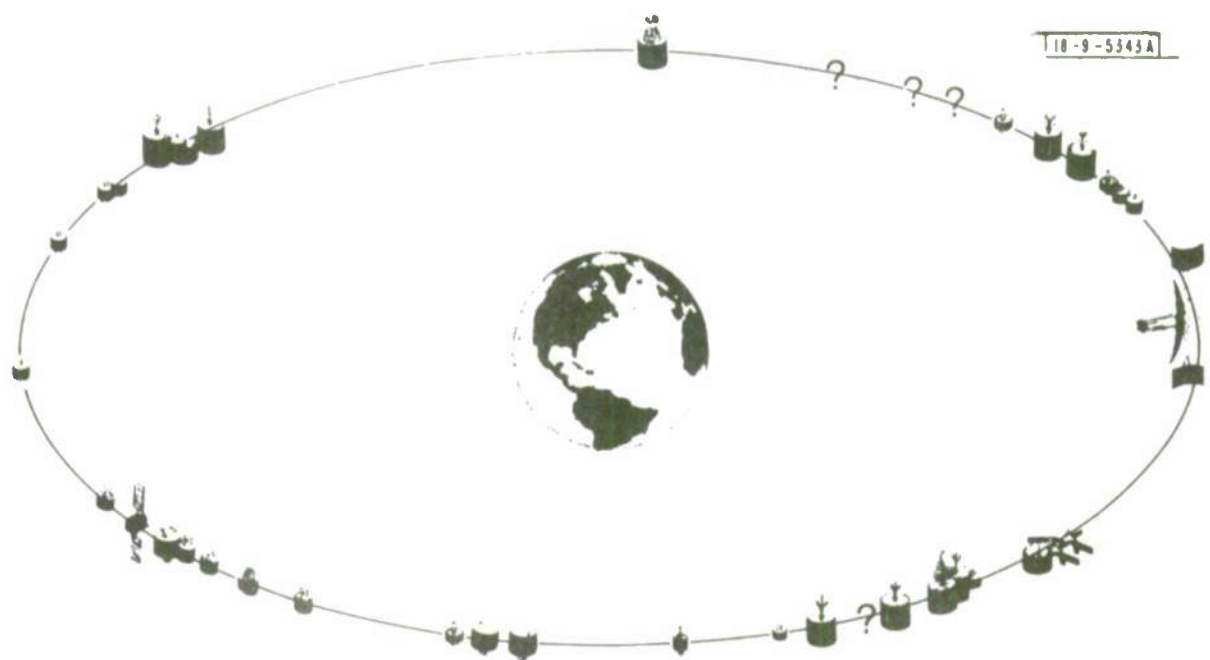
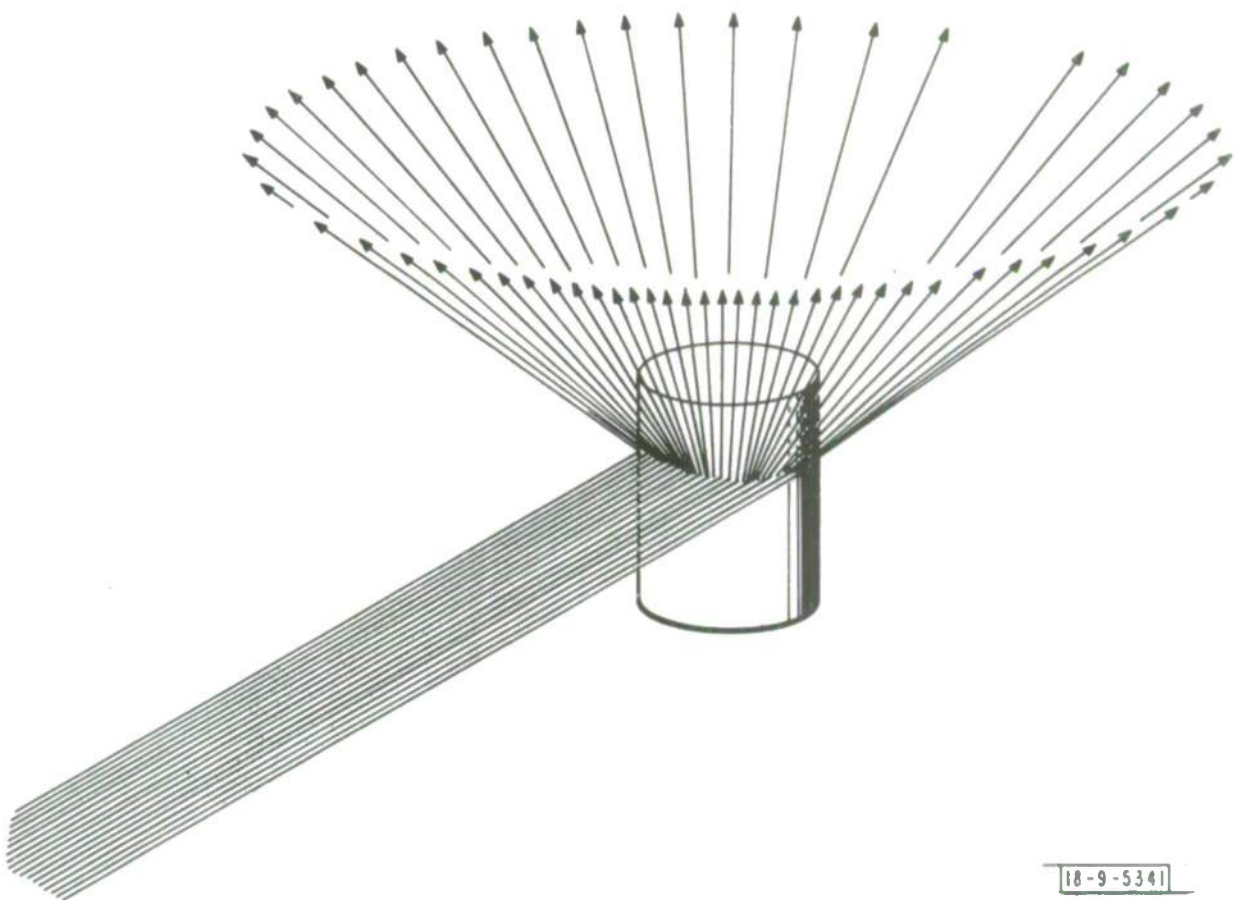


Fig. 5. Geosynchronous satellites launched before 1 January 1976
[Adapted from Comsat Technical Review, vol. 6, no. 1, pp. 196-197]



18-9-5341

Fig. 6. Specular reflection from a cylinder (close up view)

18-9-5325



Fig. 7. Specular reflection from a cylinder



Fig. 8. Solar specular reflection from a cylinder (not to scale)

18-9-5339-A

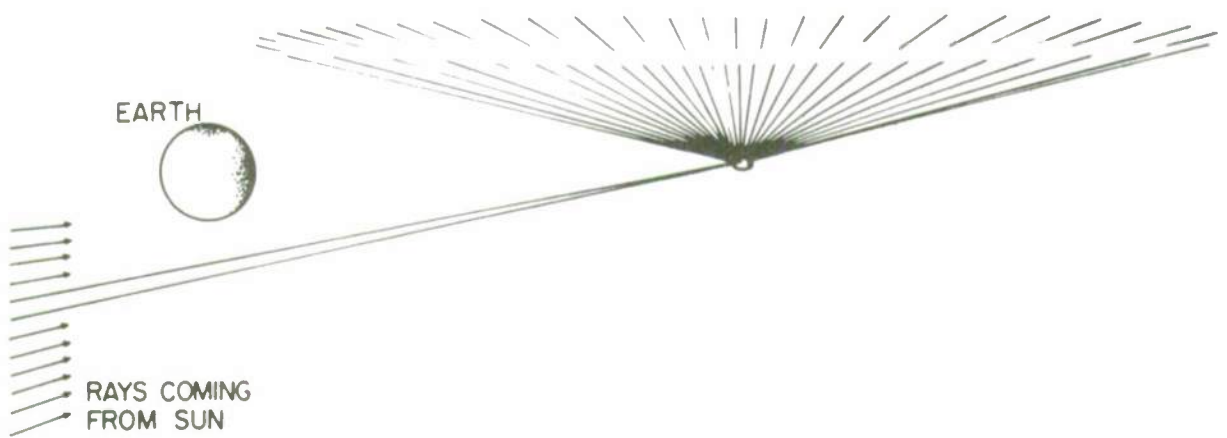


Fig. 9. Terrestrial visibility of solar specular reflection (unfavorable solar declination)

earth's. The sun's declination is such that no specularly reflected rays reach the terrestrial observer. In Figure 10, however, the opposite case is shown, only the rays striking the earth being included. According to the indicated trigonometric relationships, specular reflections are observable at a site of latitude ϕ and sub-satellite longitude if and only if the declination of the source, δ , satisfies the following equation:

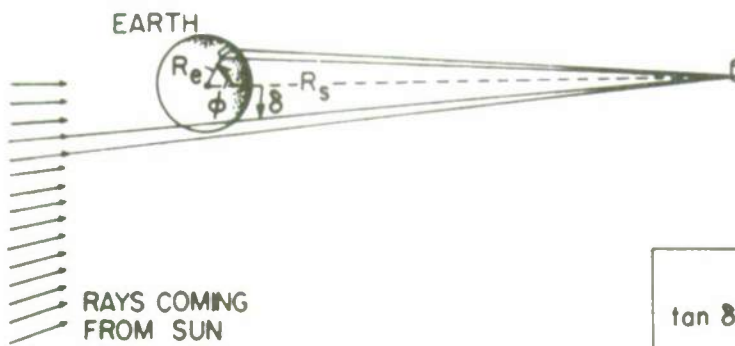
$$\tan \delta = \frac{\sin \phi}{\cos \phi - (R_s/R_e)}, \quad (A)$$

where $R_s \approx 42,164$ km is geosynchronous distance, $R_e \approx 6,378$ km is the earth's radius, and hence $(R_s/R_e) \approx 6.61$. Since the source may be any location on the sun's disk, equation (A) is equivalent to the following constraint on solar declination, δ :

$$\left| \delta - \arctan \left(\frac{\sin \phi}{\cos \phi - 6.61} \right) \right| \leq 0.5^\circ. \quad (B)$$

Hence, specular reflections are observable at just those times when δ assumes values in a specific interval, functionally related to site latitude.

The cyclic variation of solar declination is an aspect of the annual course of the seasons, as shown in Figure 11. As a result, each value of solar declination corresponds to two dates. When ϕ is restricted to northern temperate latitudes, for example, the limitations on δ imposed by equation (B) are seen to confine specular observability



$$\tan \delta = \frac{\sin \phi}{\cos \phi - (R_s / R_E)}$$

Fig. 10. Terrestrial visibility of solar specular reflection (favorable solar declination)

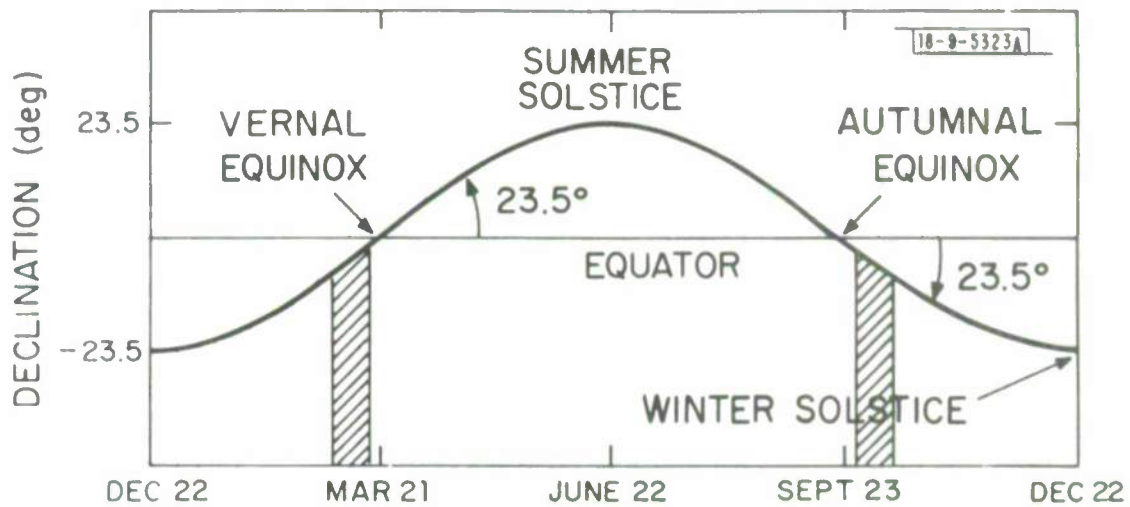


Fig. 11. Annual cycle of solar declination

to one period shortly before the vernal equinox and another shortly after the autumnal, each lasting less than two weeks. The mean rate of change of δ , then being about $.38^{\circ}/\text{day}$, the duration of specular observability at any individual site will be approximately 32 hours, part of which will occur during daylight.

Although in the real world the above simplifying assumptions do not hold, the following valid conclusion can be drawn: at a north temperate zone site (such as the Lincoln Laboratory GEODSS Test Site), specular reflections will be prevalent around the time of the equinoxes, particularly before the vernal and after the autumnal. As a corollary, if system detection capability is to be tested under least favorable brightness conditions, sensitivity measurements should be taken near the summer solstice.

A more accurate model of specular timing must take account of all deviations of the satellite orbital elements from true geosynchronous. Likewise, variations in spin axis orientation (also called attitude) must be considered. Satellites which are not perfectly balanced may in addition seem to wobble, as shown in Figure 12. This motion represents a misalignment of the cylinder's spin axis and symmetry axis, which can significantly lengthen the specular viewing period.

The above computational requirements can best be satisfied by a computer program. If it is to serve as a practical planning tool, it must be readily accessible at each GEODSS site, and its results must be provided in a convenient format. The author has written such a program

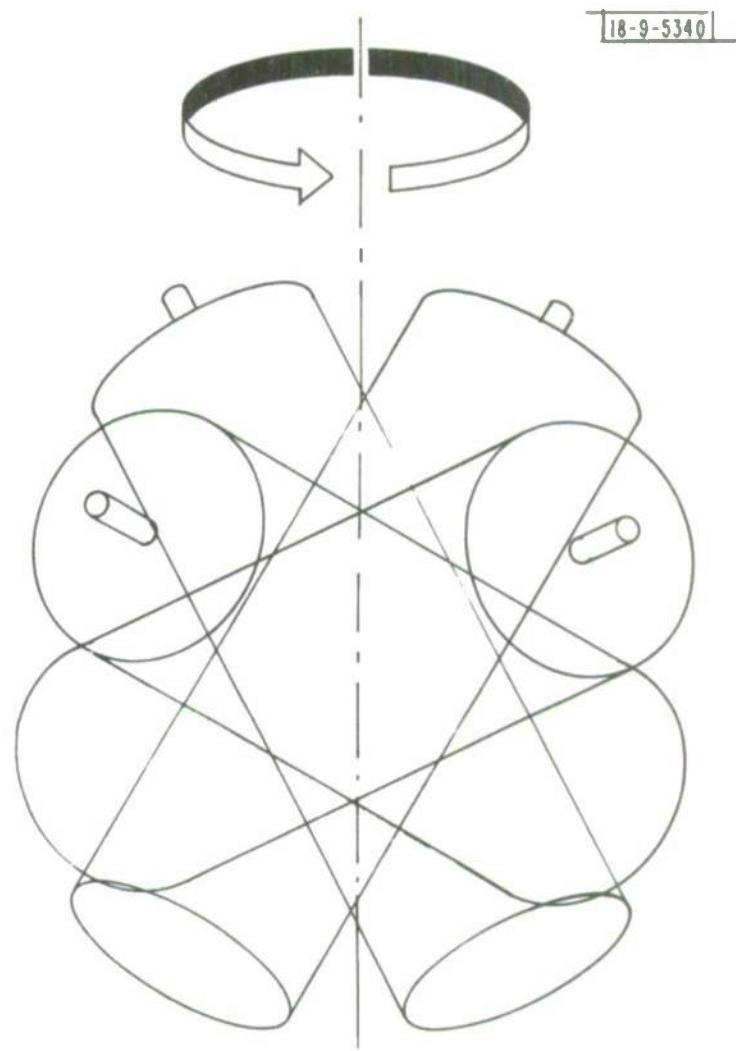


Fig. 12. Wobbling cylinder (spin axis and symmetry axis misaligned)

for the MODCOMP IV minicomputer, an example of whose output is shown in Figure 13. It takes the form of a graphic table, each row representing an observing night, each column an observing time, at ten minute intervals. In addition to observable specular reflections, indicated by (*), the chart specifies the following phenomena: sunset/sunrise (S), twilight (T), eclipse by earth (E), and (for satellites with strong sublongitude drift) descent below horizon (X). The program is interactive and command structured. The computation of a month's specular reflections takes under a minute.

The chart in Figure 13 refers to the true geosynchronous case described above, as seen from a site of latitude 35° and longitude 0° . Figures 14-16 illustrate timing changes resulting from the alteration of a single parameter. The respective modifications are: site moved to latitude 25° ; orbital inclination of 0.5° introduced; axial offset of 0.2° introduced.

When the orbital elements or other parameters are not known exactly, the specular predictions will also contain uncertainty. For example, a change of 0.1° in inclination may cause a shift of as much as six hours in specular observability, and a like change in attitude may have a 12 hour response. When the objective is to recognize a satellite by its known diffuse return, a reasonable precaution is to augment the predicted specular period by a buffer period incorporating recognized uncertainty. When the objective is to capitalize on specular brightness for detection, one should schedule observations near the center of the longest specular

SATELLITE ORBITAL ELEMENTS FROM CYCLOMUSOL SPINNING, SPIN AXIS = SYMMETRY 6810
TURBO, USE SITES LADS
UNITS: HYPOTHETICAL GEOSTATIONARY SATELLITE

-9-5425

EPOLINE 1976 ZOD 01 01 0.0
No 1.01277905 AM 6.6105 LE 0.000000 IE 0.0000
ORBIT 0.0000 EQUATOR 0.0000 RA 0.0000
HJD 2451000 MEAN ANG 0.00 ULLAGE 90.00 ROLL/INCL 0.00
OFFSET FROM CHM HUMBLE 0.00 LONG FROM ANGUS 0.00

SATELLITE GRAPHIC TIME TABLE
FROM SEP 1976 THROUGH NOV 1976

	16	17	18	19	20	21	22	23	24	25	26	27	28	29	30	31	1	2	3	4	5	6	7	8
*1976																								
1	011	012	013	014	015	016	017	018	019	01A	01B	01C	01D	01E	01F	01G	01H	01I	01J	01K	01L	01M	01N	
2	01P	01Q	01R	01S	01T	01U	01V	01W	01X	01Y	01Z	02A	02B	02C	02D	02E	02F	02G	02H	02I	02J	02K	02L	02M
3	02P	02Q	02R	02S	02T	02U	02V	02W	02X	02Y	02Z	03A	03B	03C	03D	03E	03F	03G	03H	03I	03J	03K	03L	03M
4	03P	03Q	03R	03S	03T	03U	03V	03W	03X	03Y	03Z	04A	04B	04C	04D	04E	04F	04G	04H	04I	04J	04K	04L	04M
5	04P	04Q	04R	04S	04T	04U	04V	04W	04X	04Y	04Z	05A	05B	05C	05D	05E	05F	05G	05H	05I	05J	05K	05L	05M
6	05P	05Q	05R	05S	05T	05U	05V	05W	05X	05Y	05Z	06A	06B	06C	06D	06E	06F	06G	06H	06I	06J	06K	06L	06M
7	06P	06Q	06R	06S	06T	06U	06V	06W	06X	06Y	06Z	07A	07B	07C	07D	07E	07F	07G	07H	07I	07J	07K	07L	07M
8	07P	07Q	07R	07S	07T	07U	07V	07W	07X	07Y	07Z	08A	08B	08C	08D	08E	08F	08G	08H	08I	08J	08K	08L	08M
9	08P	08Q	08R	08S	08T	08U	08V	08W	08X	08Y	08Z	09A	09B	09C	09D	09E	09F	09G	09H	09I	09J	09K	09L	09M
10	09P	09Q	09R	09S	09T	09U	09V	09W	09X	09Y	09Z	0A0	0A1	0A2	0A3	0A4	0A5	0A6	0A7	0A8	0A9	0A0	0A1	0A2
11	0A3	0A4	0A5	0A6	0A7	0A8	0A9	0A0	0A1	0A2	0A3	0A4	0A5	0A6	0A7	0A8	0A9	0A0	0A1	0A2	0A3	0A4	0A5	0A6
12	0A7	0A8	0A9	0A0	0A1	0A2	0A3	0A4	0A5	0A6	0A7	0A8	0A9	0A0	0A1	0A2	0A3	0A4	0A5	0A6	0A7	0A8	0A9	0A0
13	0A1	0A2	0A3	0A4	0A5	0A6	0A7	0A8	0A9	0A0	0A1	0A2	0A3	0A4	0A5	0A6	0A7	0A8	0A9	0A0	0A1	0A2	0A3	0A4
14	0A5	0A6	0A7	0A8	0A9	0A0	0A1	0A2	0A3	0A4	0A5	0A6	0A7	0A8	0A9	0A0	0A1	0A2	0A3	0A4	0A5	0A6	0A7	0A8
15	0A9	0A0	0A1	0A2	0A3	0A4	0A5	0A6	0A7	0A8	0A9	0A0	0A1	0A2	0A3	0A4	0A5	0A6	0A7	0A8	0A9	0A0	0A1	0A2
16	0A3	0A4	0A5	0A6	0A7	0A8	0A9	0A0	0A1	0A2	0A3	0A4	0A5	0A6	0A7	0A8	0A9	0A0	0A1	0A2	0A3	0A4	0A5	0A6
17	0A7	0A8	0A9	0A0	0A1	0A2	0A3	0A4	0A5	0A6	0A7	0A8	0A9	0A0	0A1	0A2	0A3	0A4	0A5	0A6	0A7	0A8	0A9	0A0
18	0A1	0A2	0A3	0A4	0A5	0A6	0A7	0A8	0A9	0A0	0A1	0A2	0A3	0A4	0A5	0A6	0A7	0A8	0A9	0A0	0A1	0A2	0A3	0A4
19	0A5	0A6	0A7	0A8	0A9	0A0	0A1	0A2	0A3	0A4	0A5	0A6	0A7	0A8	0A9	0A0	0A1	0A2	0A3	0A4	0A5	0A6	0A7	0A8
20	0A9	0A0	0A1	0A2	0A3	0A4	0A5	0A6	0A7	0A8	0A9	0A0	0A1	0A2	0A3	0A4	0A5	0A6	0A7	0A8	0A9	0A0	0A1	0A2
21	0A3	0A4	0A5	0A6	0A7	0A8	0A9	0A0	0A1	0A2	0A3	0A4	0A5	0A6	0A7	0A8	0A9	0A0	0A1	0A2	0A3	0A4	0A5	0A6
22	0A7	0A8	0A9	0A0	0A1	0A2	0A3	0A4	0A5	0A6	0A7	0A8	0A9	0A0	0A1	0A2	0A3	0A4	0A5	0A6	0A7	0A8	0A9	0A0
23	0A1	0A2	0A3	0A4	0A5	0A6	0A7	0A8	0A9	0A0	0A1	0A2	0A3	0A4	0A5	0A6	0A7	0A8	0A9	0A0	0A1	0A2	0A3	0A4
24	0A5	0A6	0A7	0A8	0A9	0A0	0A1	0A2	0A3	0A4	0A5	0A6	0A7	0A8	0A9	0A0	0A1	0A2	0A3	0A4	0A5	0A6	0A7	0A8
25	0A9	0A0	0A1	0A2	0A3	0A4	0A5	0A6	0A7	0A8	0A9	0A0	0A1	0A2	0A3	0A4	0A5	0A6	0A7	0A8	0A9	0A0	0A1	0A2
26	0A3	0A4	0A5	0A6	0A7	0A8	0A9	0A0	0A1	0A2	0A3	0A4	0A5	0A6	0A7	0A8	0A9	0A0	0A1	0A2	0A3	0A4	0A5	0A6
27	0A7	0A8	0A9	0A0	0A1	0A2	0A3	0A4	0A5	0A6	0A7	0A8	0A9	0A0	0A1	0A2	0A3	0A4	0A5	0A6	0A7	0A8	0A9	0A0
28	0A1	0A2	0A3	0A4	0A5	0A6	0A7	0A8	0A9	0A0	0A1	0A2	0A3	0A4	0A5	0A6	0A7	0A8	0A9	0A0	0A1	0A2	0A3	0A4
29	0A5	0A6	0A7	0A8	0A9	0A0	0A1	0A2	0A3	0A4	0A5	0A6	0A7	0A8	0A9	0A0	0A1	0A2	0A3	0A4	0A5	0A6	0A7	0A8
30	0A9	0A0	0A1	0A2	0A3	0A4	0A5	0A6	0A7	0A8	0A9	0A0	0A1	0A2	0A3	0A4	0A5	0A6	0A7	0A8	0A9	0A0	0A1	0A2
*1976																								
1	011	012	013	014	015	016	017	018	019	01A	01B	01C	01D	01E	01F	01G	01H	01I	01J	01K	01L	01M	01N	
2	01P	01Q	01R	01S	01T	01U	01V	01W	01X	01Y	01Z	02A	02B	02C	02D	02E	02F	02G	02H	02I	02J	02K	02L	02M
3	02P	02Q	02R	02S	02T	02U	02V	02W	02X	02Y	02Z	03A	03B	03C	03D	03E	03F	03G	03H	03I	03J	03K	03L	03M
4	03P	03Q	03R	03S	03T	03U	03V	03W	03X	03Y	03Z	04A	04B	04C	04D	04E	04F	04G	04H	04I	04J	04K	04L	04M
5	04P	04Q	04R	04S	04T	04U	04V	04W	04X	04Y	04Z	05A	05B	05C	05D	05E	05F	05G	05H	05I	05J	05K	05L	05M
6	05P	05Q	05R	05S	05T	05U	05V	05W	05X	05Y	05Z	06A	06B	06C	06D	06E	06F	06G	06H	06I	06J	06K	06L	06M
7	06P	06Q	06R	06S	06T	06U	06V	06W	06X	06Y	06Z	07A	07B	07C	07D	07E	07F	07G	07H	07I	07J	07K	07L	07M
8	07P	07Q	07R	07S	07T	07U	07V	07W	07X	07Y	07Z	08A	08B	08C	08D	08E	08F	08G	08H	08I	08J	08K	08L	08M
9	08P	08Q	08R	08S	08T	08U	08V	08W	08X	08Y	08Z	09A	09B	09C	09D	09E	09F	09G	09H	09I	09J	09K	09L	09M
10	09P	09Q	09R	09S	09T	09U	09V	09W	09X	09Y	09Z	0A0	0A1	0A2	0A3	0A4	0A5	0A6	0A7	0A8	0A9	0A0	0A1	0A2
11	0A3	0A4	0A5	0A6	0A7	0A8	0A9	0A0	0A1	0A2	0A3	0A4	0A5	0A6	0A7	0A8	0A9	0A0	0A1	0A2	0A3	0A4	0A5	0A6
12	0A7	0A8	0A9	0A0	0A1	0A2	0A3	0A4	0A5	0A6	0A7	0A8	0A9	0A0	0A1	0A2	0A3	0A4	0A5	0A6	0A7	0A8	0A9	0A0
13	0A1	0A2	0A3	0A4	0A5	0A6	0A7	0A8	0A9	0A0	0A1	0A2	0A3	0A4	0A5	0A6	0A7	0A8	0A9	0A0	0A1	0A2	0A3	0A4
14	0A5	0A6	0A7	0A8	0A9	0A0	0A1	0A2	0A3	0A4	0A5	0A6	0A7	0A8	0A9	0A0	0A1	0A2	0A3	0A4	0A5	0A6	0A7	0A8
15	0A9	0A0	0A1	0A2	0A3	0A4	0A5	0A6	0A7	0A8	0A9	0A0	0A1	0A2	0A3	0A4	0A5	0A6	0A7	0A8	0A9	0A0	0A1	0A2
16	0A3	0A4	0A5	0A6	0A7	0A8	0A9	0A0	0A1	0A2	0A3	0A4	0A5	0A6	0A7	0A8	0A9	0A0	0A1	0A2	0A3	0A4	0A5	0A6
17	0A7	0A8	0A9	0A0	0A1	0A2	0A3	0A4	0A5	0A6	0A7	0A8	0A9	0A0	0A1	0A2	0A3	0A4	0A5	0A6	0A7	0A8	0A9	0A0
18	0A1	0A2	0A3	0A4	0A5	0A6	0A7	0A8	0A9	0A0	0A1	0A2	0A3	0A4	0A5	0A6	0A7	0A8	0A9	0A0	0A1	0A2	0A3	0A4
19	0A5	0A6	0A7	0A8	0A9	0A0	0A1	0A2	0A3	0A4	0A5	0A6	0A7	0A8	0A9	0A0	0A1	0A2	0A3	0A4	0A5	0A6	0A7	0A8
20	0A9	0A0	0A1	0A2	0A3	0A4	0A5	0A6	0A7	0A8	0A9	0A0	0A1	0A2	0A3	0A4	0A5	0A6	0A7	0A8	0A9	0A0	0A1	0A2
21	0A3	0A4	0A5	0A6	0A7	0A8	0A9	0A0	0A1	0A2	0A3	0A4	0A5	0A6	0A7	0								

SPELLEIAN REFLECTION FROM CYLINDRICAL SATELLITE. SPIN AXIS = STARBOARD AXIS
TUNED. USA SIGHT LINE
OLST-1 HYDROGEN FILLED GEOSTATIONARY SATELLITE

-9-3424

LPU012 1975 dec 01 01 0.0
N 0.00211909 E 0.00185 L 0.0000000 I 0.00000

KNUJED 1.00 KARDE 0.20 WECAIR 90.00 RIBALONAKH 0.55
URFET FROM UNO NUMBER 0000 LONG FROM ANUWEN 8088

SATELLITE SHAPING TIME TABLE
FROM SEP 1973 THROUGH NOV 1978

SUSPENSE/SUNRISE
TWILIGHT
SPECULAR REFLECTION AT SITE
ECLIPSE AT EARTH
EARTHLESS THAN 8 WKS

Fig. 14. Specular reflection visibility chart (change in site latitude of 10°)

SPECULAR REFLECTION FROM CYLINDRICAL SATELLITE. SWIN AXIS = SYMMETRY AXES
FLUID. USA SITE: LA35
UNSTABLE HYDROSTATIC SEISMALMUNUS SATELLITE

- 9 - 5423

ԵՐԱՎԵՐ 1978 ՀԾ ՍԻ ՍԻ ԱՍ
ԽԸ ԼՂԴՀԴԴԴԴ ՇՈ ՏԵՎԵԱ
ԱԽՈՒՅ ԽԱ.ԱԽՈՒՅ ԽԵՎԵԿ Ս.ԱԽՈՒՅ
ԽԵՎԵԿ Ս.ԱԽՈՒՅ ԽԵՎԵԿ Ս.ԱԽՈՒՅ
ԽԵՎԵԿ Ս.ԱԽՈՒՅ ԽԵՎԵԿ Ս.ԱԽՈՒՅ

SATELLITE GRAPHIC TIME TABLE
FROM SEP 1975 THROUGH NOV 1975

S=SUNSET/SUNRISE
I=TWILIGHT
•=SPECULAR REFLECTION AT BITE
E=ECLIMBED WT EARTH
X=ALTITUDE LESS THAN 0 DEG

Fig. 15. Specular reflection visibility chart (change in orbital inclination of 0.5°)

SPALLAN REFLECTION FROM LITHONIUM SATELLITE. SWIN AXIS & SYMMETRY SWIN
LEVELS USA SITE L-38
DEBTTA HYDROXYLIC GLUTATHIONOUS SATELLITE

MHJDADS 10000 MHDADS 90000 MHDADS 80000 MHDADS 80000
OFFSET FROM END NUMBER 0.20 LENGTH FROM ANODE 90.98

9-422

SATELLITE GRAPHIC TIME TABLE
FROM SEP 1973 THROUGH NOV 1976

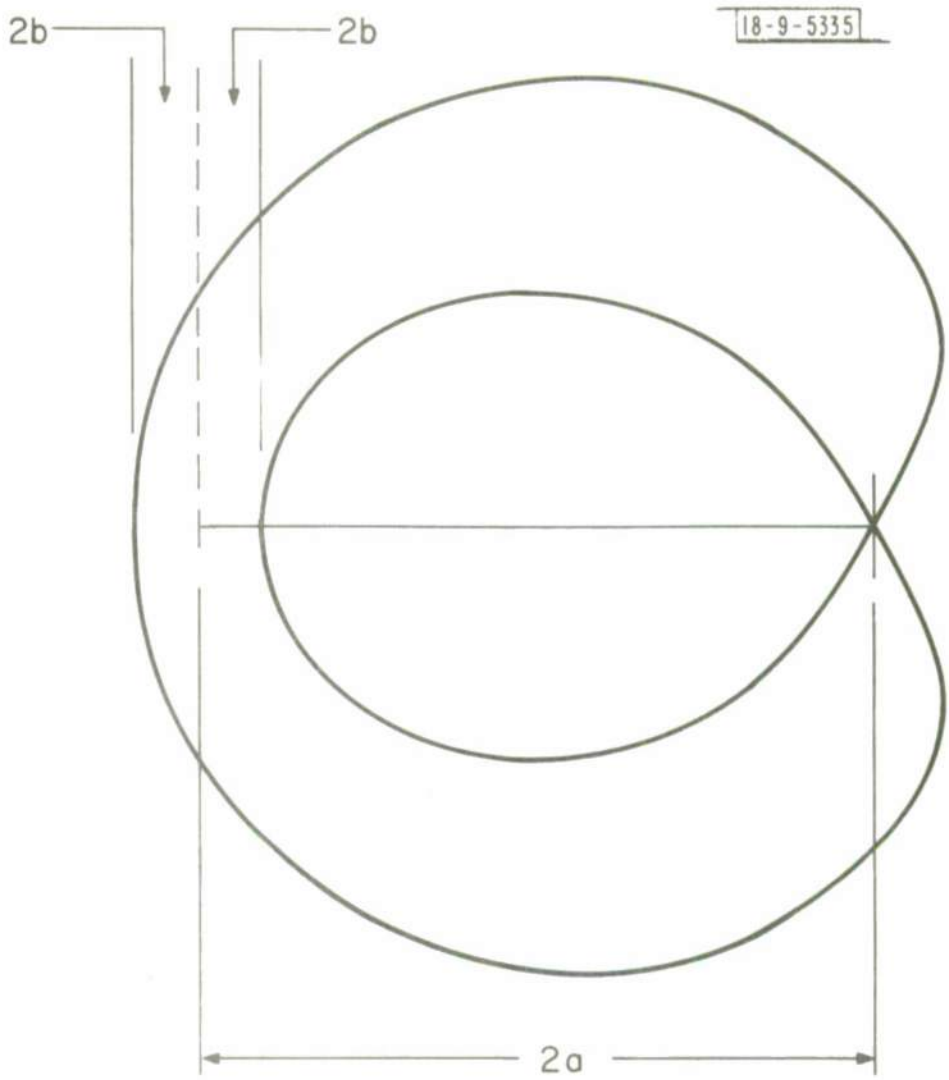
SUNSET/SUNRISE
EQUILIBRIUM
SPECULAR REFLECTION AT SITE
ECLIPSED AT EARTH
NOT LESS THAN 0.1%

Fig. 16. Specular reflection visibility chart (change in satellite attitude of 0.2°) 22

periods available. In either case, the program facilitates tentative parameter modification, so that alternate predictions may be obtained for comparison.

The case of the wobbling satellite deserves further comment. As the satellite spins about a fixed axis, its symmetry axis revolves about that spin axis because of their misalignment. As a result, the geometric requirements for specular reflection may be satisfied during some portions of a spin period and unsatisfied during others. The relevant concept is the envelope of all specular rays which may periodically be reflected. This envelope is closely related to the classical limacon of Pascal (cf. Figure 17) and can be described by a closed parametric formula. The shape of the resulting envelope is approximated in Figure 18. It still resembles a thickened cone, but the thickening is uneven and depends upon the amount of misalignment. Figure 19 shows our standard example with an introduced misalignment of 0.5° . Figure 20 shows a less artificial example, with orbital inclination of 5.7° , offset of 2.8° , and misalignment of 0.5° .

Extensive observations based on the above analysis are planned for the 1976 autumnal equinox. Already at hand are data from February and March, 1976, concerning Lincoln Experimental Satellite 6. LES-6 is particularly interesting because of its large misalignment of 2.2° and its unfavorable altitude at the Lincoln GEODSS site of less than 12° above the horizon. Pronounced specular returns were obtained at the times indicated in Figure 21, which are quite compatible with predicted



$$r = 2(b - a \cos \theta)$$

$$(x^2 + y^2 + 2ax)^2 = 4b^2(x^2 + y^2)$$

Fig. 17. Limaçon of Pascal

18-9-5339-A C

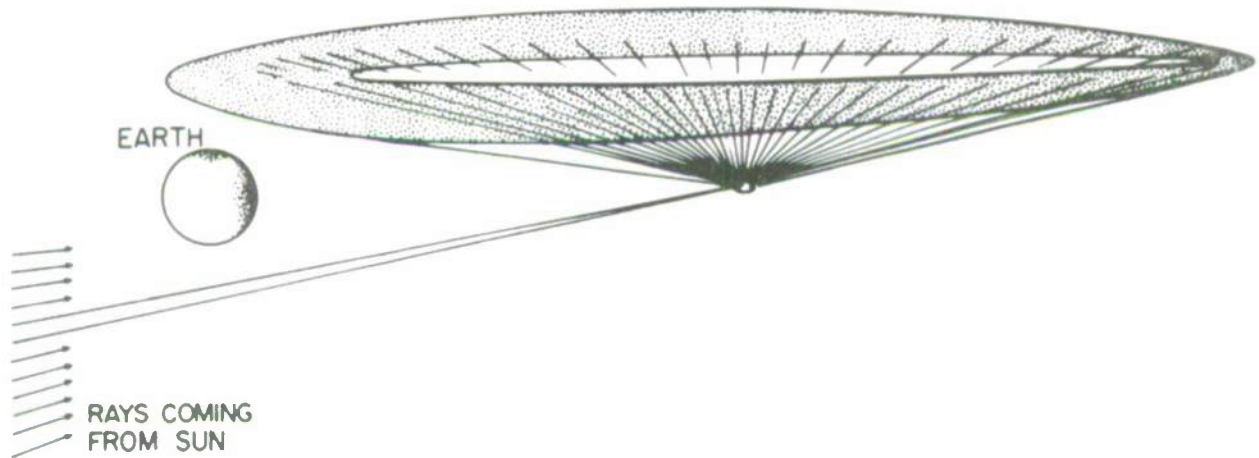


Fig. 18. Terrestrial visibility of solar specular reflection (wobbling satellite)

SPECULAR REFLECTION FROM CYLINDRICAL SATELLITE: SPIN AXIS AND SYMMETRY AXIS MISALIGNED
 TURBO USA BITE LASS
 ULETTI HYPOTHETICAL GEOSYNCHRONOUS SATELLITE

-9-5421

EPOCH: 1976 065 01 01 00.0
 NO. 1,04277945 AZ 0.6105 E 0.0000000 ID 0.0000
 ANGLES 0.0000 4KWPMS 0.0000 ME 0.0000
 KNOB: 1.00 MAXE 0.00 DECAE 90.00 MISALIGNAB: 0.50
 OFFSET FROM ORB NORMS 0.00 LONG FROM ANGLES 0.00

SATELLITE GRAPHIC TIME TABLE
 FROM SEP 1976 THROUGH NOV 1976

	16	17	18	19	20	21	22	23	24	25	26	27	28	29	30	31	1	2	3	4	5	6	7	8
	LOCAL MEAN SOLAR TIME												1976											
*1976																								
1 SEP 245	1	1	b	1	T1	1	1	1	E1E1	1	1	1	T	1	S	1							2 SEP 246	
2 SEP 246	1	1	a	1	T1	1	1	1	E1E1	1	1	1	S	1									3 SEP 247	
3 SEP 247	1	1	a	1	T1	1	1	1	E1E1	1	1	1	S	1									4 SEP 248	
4 SEP 248	1	1	a	1	T1	1	1	1	E1E1	1	1	1	S	1									5 SEP 249	
5 SEP 249	1	1	a	1	T1	1	1	1	E1E1	1	1	1	S	1									6 SEP 250	
6 SEP 250	1	1	a	1	T1	1	1	1	E1E1	1	1	1	S	1									7 SEP 251	
7 SEP 251	1	1	a	1	T1	1	1	1	E1E1	1	1	1	S	1									8 SEP 252	
8 SEP 252	1	1	a	1	T1	1	1	1	E1E1	1	1	1	S	1									9 SEP 253	
9 SEP 253	1	1	a	1	T1	1	1	1	E1E1	1	1	1	S	1									10 SEP 254	
10 SEP 254	1	1	a	1	T1	1	1	1	E1E1	1	1	1	S	1									11 SEP 255	
11 SEP 255	1	1	a	1	T1	1	1	1	E1E1	1	1	1	S	1									12 SEP 256	
12 SEP 256	1	1	a	1	T1	1	1	1	E1E1	1	1	1	S	1									13 SEP 257	
13 SEP 257	1	1	a	1	T1	1	1	1	E1E1	1	1	1	S	1									14 SEP 258	
14 SEP 258	1	1	a	1	T1	1	1	1	E1E1	1	1	1	S	1									15 SEP 259	
15 SEP 259	1	1	a	1	T1	1	1	1	E1E1	1	1	1	S	1									16 SEP 260	
16 SEP 260	1	1	a	1	T1	1	1	1	E1E1	1	1	1	S	1									17 SEP 261	
17 SEP 261	1	1	a	1	T1	1	1	1	E1E1	1	1	1	S	1									18 SEP 262	
18 SEP 262	1	1	a	1	T1	1	1	1	E1E1	1	1	1	S	1									19 SEP 263	
19 SEP 263	1	1	a	1	T1	1	1	1	E1E1	1	1	1	S	1									20 SEP 264	
20 SEP 264	1	1	a	1	T1	1	1	1	E1E1	1	1	1	S	1									21 SEP 265	
21 SEP 265	1	1	a	1	T1	1	1	1	E1E1	1	1	1	S	1									22 SEP 266	
22 SEP 266	1	1	a	1	T1	1	1	1	E1E1	1	1	1	S	1									23 SEP 267	
23 SEP 267	1	1	a	1	T1	1	1	1	E1E1	1	1	1	S	1									24 SEP 268	
24 SEP 268	1	1	a	1	T1	1	1	1	E1E1	1	1	1	S	1									25 SEP 269	
25 SEP 269	1	1	a	1	T1	1	1	1	E1E1	1	1	1	S	1									26 SEP 270	
26 SEP 270	1	1	a	1	T1	1	1	1	E1E1	1	1	1	S	1									27 SEP 271	
27 SEP 271	1	1	a	1	T1	1	1	1	E1E1	1	1	1	S	1									28 SEP 272	
28 SEP 272	1	1	a	1	T1	1	1	1	E1E1	1	1	1	S	1									29 SEP 273	
29 SEP 273	1	1	a	1	T1	1	1	1	E1E1	1	1	1	S	1									30 SEP 274	
30 SEP 274	1	1	a	1	T1	1	1	1	E1E1	1	1	1	S	1									1 OCT 275	
*1976																								
1 OCT 276	1	1	a	1	T1	1	1	1	E1E1	1	1	1	S	1									2 OCT 276	
2 OCT 277	1	1	a	1	T1	1	1	1	E1E1	1	1	1	S	1									3 OCT 278	
3 OCT 278	1	1	a	1	T1	1	1	1	E1E1	1	1	1	S	1									4 OCT 279	
5 OCT 279	1	1	a	1	T1	1	1	1	E1E1	1	1	1	S	1									6 OCT 280	
6 OCT 280	1	1	a	1	T1	1	1	1	E1E1	1	1	1	S	1									7 OCT 281	
7 OCT 281	1	1	a	1	T1	1	1	1	E1E1	1	1	1	S	1									8 OCT 282	
9 OCT 282	1	1	a	1	T1	1	1	1	E1E1	1	1	1	S	1									10 OCT 283	
10 OCT 283	1	1	a	1	T1	1	1	1	E1E1	1	1	1	S	1									11 OCT 284	
11 OCT 284	1	1	a	1	T1	1	1	1	E1E1	1	1	1	S	1									12 OCT 285	
12 OCT 285	1	1	a	1	T1	1	1	1	E1E1	1	1	1	S	1									13 OCT 286	
13 OCT 286	1	1	a	1	T1	1	1	1	E1E1	1	1	1	S	1									14 OCT 288	
14 OCT 288	1	1	a	1	T1	1	1	1	E1E1	1	1	1	S	1									15 OCT 289	
15 OCT 289	1	1	a	1	T1	1	1	1	E1E1	1	1	1	S	1									16 OCT 290	
17 OCT 290	1	1	a	1	T1	1	1	1	E1E1	1	1	1	S	1									17 OCT 291	
18 OCT 291	1	1	a	1	T1	1	1	1	E1E1	1	1	1	S	1									18 OCT 292	
19 OCT 292	1	1	a	1	T1	1	1	1	E1E1	1	1	1	S	1									19 OCT 293	
20 OCT 293	1	1	a	1	T1	1	1	1	E1E1	1	1	1	S	1									21 OCT 295	
22 OCT 295	1	1	a	1	T1	1	1	1	E1E1	1	1	1	S	1									23 OCT 296	
23 OCT 296	1	1	a	1	T1	1	1	1	E1E1	1	1	1	S	1									24 OCT 297	
24 OCT 297	1	1	a	1	T1	1	1	1	E1E1	1	1	1	S	1									25 OCT 298	
25 OCT 298	1	1	a	1	T1	1	1	1	E1E1	1	1	1	S	1									26 OCT 299	
26 OCT 299	1	1	a	1	T1	1	1	1	E1E1	1	1	1	S	1									27 OCT 301	
27 OCT 301	1	1	a	1	T1	1	1	1	E1E1	1	1	1	S	1									28 OCT 302	
28 OCT 302	1	1	a	1	T1	1	1	1	E1E1	1	1	1	S	1									29 OCT 303	
29 OCT 303	1	1	a	1	T1	1	1	1	E1E1	1	1	1	S	1									30 OCT 304	
30 OCT 304	1	1	a	1	T1	1	1	1	E1E1	1	1	1	S	1									31 OCT 305	
31 OCT 305	1	1	a	1	T1	1	1	1	E1E1	1	1	1	S	1									1 NOV 306	
*1976																								
1 NOV 306	1	1	a	1	T1	1	1	1	E1E1	1	1	1	S	1									2 NOV 307	
2 NOV 307	1	1	a	1	T1	1	1	1	E1E1	1	1	1	S	1									3 NOV 308	
4 NOV 309	1	1	a	1	T1	1	1	1	E1E1	1	1	1	S	1									5 NOV 309	
5 NOV 310	1	1	a	1	T1	1	1	1	E1E1	1	1	1	S	1									6 NOV 311	
6 NOV 311	1	1	a	1	T1	1	1	1	E1E1	1	1	1	S	1									7 NOV 312	
7 NOV 312	1	1	a	1	T1	1	1	1	E1E1	1	1	1	S	1									8 NOV 313	
8 NOV 313	1	1	a	1	T1	1	1	1	E1E1	1	1	1	S	1									9 NOV 314	
10 NOV 315	1	1	a	1	T1	1	1	1	E1E1	1	1	1	S	1									11 NOV 315	
11 NOV 316	1	1	a	1	T1	1	1	1	E1E1	1	1	1	S	1									12 NOV 317	
12 NOV 317	1	1	a	1	T1	1	1	1	E1E1	1	1	1	S	1									13 NOV 318	
15 NOV 319	1	1	a	1	T1	1	1	1	E1E1	1	1	1	S	1									14 NOV 319	
15 NOV 320	1	1	a	1	T1	1	1	1	E1E1	1	1	1</td												

SPELLEER REPLICATION FROM LYRICALNICAL SATELLITE. SPIN AXIS AND STRUCTRT AXIS MISALIGNED
10000. USA SITE STAL
0001. HYDRAULIC ALARM CLOUTCHMUNIC SATELLITE

-9- 5420

DEPT OF STATE KANSAS 168.90 ULCAKES -86.75 RIBALONAKS 8.88
UPSTATE KANSAS 2.83 LONG FROM ANDOVER 87.48

SATELLITE GRAPHIC TIME TABLE
FROM SEP 1978 THROUGH NOV 1978

X=BUNST/BUNR10E
T=TaILIGHT
S=SPECULAR REFLECTION AT SITE
E=ECLIPSED BY EARTH
Z=ALTITUDE LESS THAN 2 DEG

Fig. 20. Specular reflection visibility chart (misalignment present)

SPECIFIC INFLUENCE FROM EXTRANOMIAL SATELLITE, SPIN AXIS & STRUTRY AXIS
SATELLITE USE SATELLITE SIAL
LINEAR AND LINEAR EXPERIMENTAL SATELLITE - 8 180C 84821

-9-3419

EFULHES 1976 46 131211 1.0
 43 1.0007000 ex 0.6161 1 ex 5.5000000 1 ex 8.7818
 ANUOS 60.000 ARBPCMS 105.2250 1 ex 359.981

SATELLITE GRAPHIC TIME TABLE
FROM FEB 1976 THROUGH APR 1976



Fig. 21. Specular reflection visibility chart (LES-6 - Spring, 1976)

timing. A record of unsuccessful observation attempts for similar comparison would have been most desirable and will be included in the fall observing program.

UNCLASSIFIED

SECURITY CLASSIFICATION OF THIS PAGE (When Data Entered)

